Nuclear Instruments and Methods in Physics Research A 731 (2013) 247–251

Contents lists available at ScienceDirect

Nuclear Instruments and Methods in Physics Research A

journal homepage: www.elsevier.com/locate/nima

Beam test of novel n-in-p strip sensors for high radiation environment

T. Kubota [a,*], T. Kishida [a], O. Jinnouchi [a], Y. Ikegami [b], Y. Unno [b], S. Terada [b], S. Mitsui [b], A. Tamii [c], T. Aoi [c], K. Hanagaki [d], K. Hara [e], N. Kimura [f], R. Takashima [h], Y. Takubo [b], J. Tojo [i], K. Nagai [e], I. Nakano [g], K. Yorita [f]

[a] Department of Physics, Tokyo Institute of Technology, 2-12-1 Ookayama, Meguro-ku, Tokyo 152-8550, Japan
[b] Institute of Particle and Nuclear Study, High Energy Accelerator Research Organization (KEK), 1-1 Oho, Tsukuba-shi, Ibaraki 305-0801, Japan
[c] Research Center of Nuclear Physics (RCNP), 10-1 Mihogaoka, Ibaraki, Osaka 567-0047, Japan
[d] Department of Physics, Osaka University, Machikaneyama-cho, Toyonaka-shi, Osaka 560-0043, Japan
[e] Institute of Pure and Applied Sciences, University of Tsukuba, 1-1-1 Tennoudai, Tsukuba-shi, Ibaraki 305-8571, Japan
[f] Research Institute for Science and Engineering, Waseda University, Japan
[g] Department of Physics, Okayama University, 3-1-1 Tshushima-naka, Kita-ku, Okayama-shi, Okayama 700-8530, Japan
[h] Department of Education, Kyoto University of Education, 1 Fukakusa-Fujimori-cho, Fushimi-ku, Kyoto 612-8522, Japan
[i] Department of Physics, Kyushu University, 6-10-1 Hakozaki, Higashi-ku, Fukuoka 812-8581, Japan

ARTICLE INFO

Available online 17 June 2013

Keywords:
Strip detector
SCT
n-in-p
ATLAS
HL-LHC

ABSTRACT

Highly radiation tolerant n-in-p strip sensors have been developed for the high-luminosity LHC (HL-LHC). This paper reports the results of measurements with 392 MeV kinetic energy proton beam at RCNP in December 2011. The data was taken with a new DAQ system consisting of an universal read-out board 'SEABAS' and beam tracking telescopes whose spacial resolution is better than 5 μm. The aim of this beam test is to evaluate the new 1 cm × 1 cm n-in-p miniature sensors before and after 10^{15} n_{eq} cm^{-2} irradiation. The median charge of un-irradiated sensor is 6.2 fC at full depletion voltage, while the median charge after 10^{15} n_{eq} cm^{-2} irradiation of the sensor is 4.2 fC. The novel Punch-Through-Protection (PTP) has been implemented in these sensors. The length of active region of the sensor around PTP is observed to be decreased by 12 μm in the irradiated sensors at 10^{15} n_{eq} cm^{-2}.

1. Introduction

The LHC is planned to be upgraded to HL-LHC for new physics at the high energy by improving the statistics. The goal in instantaneous luminosity is 5×10^{34} s^{-1} cm^{-2} and the goal in integrated luminosity is 3000 fb^{-1}. The increase of the integrated luminosity will make one order of magnitude larger radiation damage to the ATLAS detector [4]. This particularly important for the inner detectors. In order to keep the performance of semiconductor tracker (SCT) after the LHC upgrade, new structures of sensor and read-out chip have been developed. In this paper, we present the result of the beam test carried out at the Research Center of Nuclear Physics (RCNP) of Osaka University in December 2012 [3]. In this beam test, 'n-in-p' sensors with various irradiation level, 0 (un-irradiated), 5×10^{12}, 10^{13}, 10^{14} and 10^{15} n_{eq} cm^{-2} were tested. The n-in-p sensor has a number of advantages compared to the 'p-in-n' sensor. In the 'p-in-n' sensors the type inversion occurs at a few 10^{13} n_{eq} cm^{-2} irradiation. After the type inversion, the silicon bulk is depleted from the back side. The type inversion does not occur in the p-type silicon bulk and the depletion zone is always formed from the strip side. This advantage means that the n-in-p sensor is operational without full depletion after high irradiation. The n^+-strips collect electrons for read-out while the p^+-strips collect holes. These two features allow n-in-p sensors to have high radiation tolerance and faster read-out. To read-out n-in-p sensors for beam test, a dedicated DAQ system was developed. The system consists of new read-out chip 'ABCN' (ATLAS Binary Chip Next) [1] and universal read-out board 'SEABAS' [2]. The beam telescope, whose spacial resolution is better than 5 μm, was used with new DAQ to determine the precise track location at detectors under test (DUTs).

The aims of beam test were

- Studying the charge collection efficiency of n-in-p strip sensors with new read out chip 'ABCN'.
- Studying the behavior of the PTP structure on active regions of n-in-p strip sensors before and after irradiation.

In this paper, we describe the setup of beam test (Section 2), the run plans (Section 3) and the analysis (Section 4).

2. Setup

This beam test made use of the proton beam line facility in RCNP. The 392 MeV kinetic energy proton beam with approximately

* Corresponding author. Tel.: +81 3 5734 2388.
E-mail address: kubota@hep.phys.titech.ac.jp (T. Kubota).

0168-9002/$ - see front matter © 2013 Published by Elsevier B.V.
http://dx.doi.org/10.1016/j.nima.2013.06.005

2×3 cm^2 beam spot size was used. The setup of this beam test, illustrated in Fig. 1, consists of scintillation counters for trigger, beam telescopes and detector under the test (DUT).

2.1. Beam telescope

The beam telescope was used for beam tracking. One telescope module consists of two silicon strip sensors, and each provides X and Y space point. The strip pitch of the sensor is 50 μm and the number of strips is 384. The strip signals are multiplexed by Viking Analog chip [6] and read-out by VME flash ADC modules. The analog read-out enables the beam telescope to achieve better than 5 μm spacial resolution when the high momentum beam is injected. The dead time of the telescope is 10 ms. In this beam test, two telescope modules were used, one before DUTs and another one after DUTs shown in Fig. 1.

2.2. DUTs

The n-in-p strip sensors are manufactured by Hamamatsu Photonics (HPK) in collaboration with KEK. The miniature sensors, shown in Fig. 2, were also manufactured for the evaluation. The sensors were irradiated in various levels by 70 MeV proton at CYRIC (CYclotron and RadioIsotope Center). The specification of miniature sensors is shown in Table 1.

The miniature sensors have PTP (Punch Through Protection) structure on the end of the strip as shown in Fig. 5. The PTP structure routes the large induced current to the bias ring to protect the AC coupling capacitors. Each sensor is mounted on sensor-board as shown in Fig. 3 and connected to Single Chip Card (SCC) as shown in Fig. 4. In this beam test, only 34 strips out of 103 strips are connected to the read-out pads by wire-bonding technology. The new read-out chip 'ABCN' is mounted on the SCC. The ABCN chip has been developed for operating with the short strip, and is compatible with both signal polarities, thus the SCC can be used with both n-in-p and p-in-n sensors. The ABCN chips are read-out via TCP/IP connection by the DAQ system using the SEABAS universal read-out board. Up to eight SCCs are read-out simultaneously, and the maximum DAQ rate operating with the beam telescope is about 10 kHz while that with beam telescope is about 100 Hz.

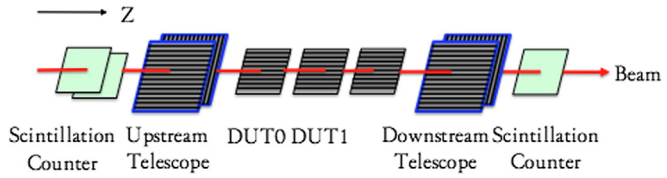

Fig. 1. The setup of beam test. The setup consists of three parts, the scintillation counters, the beam telescopes and the DUTs.

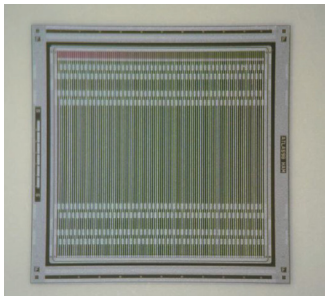

Fig. 2. Photograph of the miniature sensor. The miniature sensor contains 103 strips with 74.5 μm pitch.

3. Run plans

We operated three run plans in this beam test. The beam injection frequency was adjusted for the each run plan to match with the test condition, e.g., 10 kHz. The summary of the tested

Table 1
Features of miniature sensor.

Sensor type	FZ4D5
Size	1 cm^2 × 1 cm^2
Number of strips	103
Bonded strips	34
Strip pitch	74.5 μm
Strip length	8050 μm
Thickness	320 μm

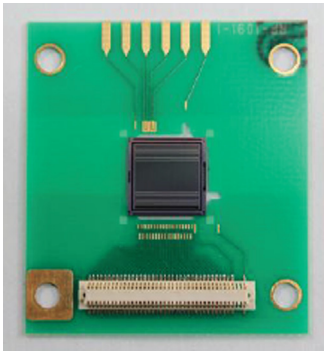

Fig. 3. Photograph of the sensor-board. The 34 strips are wire-bonded to the read-out pads.

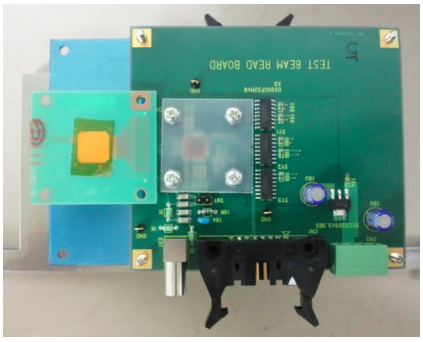

Fig. 4. Photograph of the single chip card.

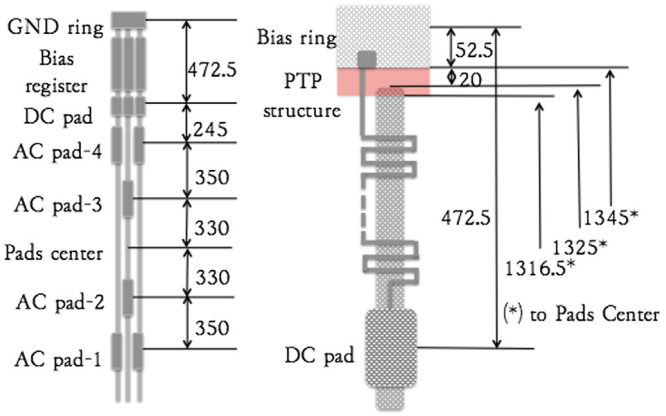

Fig. 5. Left: The schematic view of the pads position of DUT. Right: The schematic view of the strip end. The scale of length is μm.

DUTs and characteristics of them for each run plan are shown in Table 2.

Plan1. *The threshold scan of un-irradiated n-in-p and p-in-n sensors without the beam telescope.*
Plan1 was operated with two n-in-p sensors and three p-in-n sensors, aimed to measure the hit efficiencies and the collected charges of un-irradiated n-in-p sensors. For the sake of efficient data collection, beam telescope was excluded from the DAQ because of slow read-out. The un-irradiated p-in-n sensors were used as a reference in substitute of the telescope for beam tracking. In this plan, two parameters, the threshold voltage and the sensor bias voltage, were varied during the data acquisition. The threshold voltage was varied in order to measure the collected charge as the ABCN chip does not have ADC function. The median charge value is estimated by the threshold voltage whose hit efficiency is 50%. In order to convert threshold voltages (mV) into charges fC, calibrations were performed with injected charges from ABCN chip. Sensor bias voltages were varied to measure the relation between bias voltage and collected charge. Threshold voltages were varied between 96 and 800 mV in 110 steps. Bias voltages were varied between 15 and 400 V in eight steps.

Plan2. *The threshold scan of irradiated n-in-p sensors without the beam telescope.*
Plan2 was operated with four irradiated n-in-p sensors and one un-irradiated p-in-n sensor. This plan was aimed to measure the hit efficiency and the collected charge of irradiated n-in-p sensors. The irradiation levels, 5.7×10^{12}, 1.1×10^{13}, 1.2×10^{14} and 1.2×10^{15} n_{eq} cm^{-2} were tested. In order to suppress leak currents of irradiated sensors at cold temperatures, this run was operated in cold temperature between −30 and −60°C. The measurement menu were same as plan1, i.e., threshold scan and bias scan. Threshold voltages were varied between 96 and 800 mV in 110 steps. Bias voltages of 5.7×10^{12}, 1.1×10^{13}, 1.2×10^{14} n_{eq} cm^{-2} were varied from 50 to 500 V while 1.2×10^{15} n_{eq} cm^{-2} was from 400 to 950 V in 10 steps.

Plan3. *The hit efficiency map of un-irradiated and irradiated n-in-p sensors with the beam telescope.*
Plan3 was operated with un-irradiated and 1.2×10^{15} n_{eq} cm^{-2} irradiated n-in-p sensors. This plan was aimed to measure the length of active region especially the side which has PTP structure by mapping the hit efficiency for precise space points. The beam telescope was used to measure the particle positions at their intercept with the DUTs. In order to retain higher position resolution than 10 μm with the low beam energy, only two DUTs were set-up. Threshold voltages were fixed at 96 mV. The bias voltages were also fixed to full depletion voltage, to 350 V for un-irradiated, to 900 V for irradiated sensors.

Table 2
The DUT IDs of each plan.

DUT ID	Plan1	Plan2	Plan3
DUT0	p-in-n unirrad	p-in-n unirrad	n-in-p unirrad
DUT1	n-in-p unirrad	n-in-p 5.7×10^{12} n_{eq} cm^{-2}	n-in-p 1.2×10^{15} n_{eq} cm^{-2}
DUT2	n-in-p unirrad	n-in-p 1.1×10^{13} n_{eq} cm^{-2}	
DUT3	p-in-n unirrad	n-in-p 1.2×10^{14} n_{eq} cm^{-2}	
DUT4		n-in-p 1.2×10^{15} n_{eq} cm^{-2}	

4. Analysis

4.1. Plan1

In Plan1, threshold scan and bias scans were performed. Approximately 30,000 triggered events were collected for each threshold. The hit efficiencies of n-in-p sensors were calculated using beam tracks which were reconstructed by two reference p-in-n sensors (DUT0 and DUT3). The single hit clusters in all planes are required in order to reconstruct the beam track. The events were collected based on the selection criteria on the cluster size and the hit window size. The cluster size is the number of adjacent strips which had hits, the events with the clusters whose size was one and two were selected. The alignment is performed in *X*, *Y* and *Z* shift and rotations. The threshold curves of various bias voltages are shown in Fig. 6. Threshold curves are fitted by complementary error function, Erf, which takes into account the effect of the landau distribution shown as follows:

$$\mathrm{Erf}(q) = p_3(1-\mathrm{erf}(T\cdot f(T)) \quad (1)$$

$$f(T) = 1 + 0.6\cdot\tanh(-p_4\cdot T) \quad (2)$$

$$T = (q-p_1)/\left(\sqrt{2}\cdot p_2\right) \quad (3)$$

In these functions, p_1, p_2, p_3 and p_4 express the median, the width, the saturation and the skew, respectively.

The threshold voltage (fC) of 50% hit efficiency is defined as median charge. The median charges of various bias voltages are shown in Fig. 7. The saturation of the median charges of un-irradiated n-in-p sensors is measured around 6.2 fC above 250 V.

4.2. Plan2

Plan2 was aimed to compare the median charge of n-in-p sensors before and after the irradiation. The measurement and analysis methods were same as Plan1. Two lower irradiation level sensors were used as a reference to reconstruct beam tracks: (1) DUT0 (un-irradiated p-in-n) and DUT1 (5.7×10^{12} n_{eq} cm^{-2}

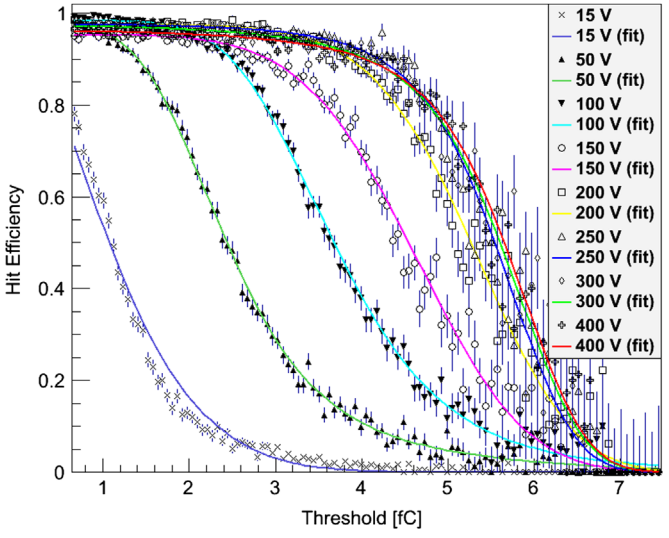

Fig. 6. The threshold curves of DUT1 in various bias voltages. The threshold voltage of 50% hit efficiency is defined as the median charge.

irradiated) and (2) DUT0 (un-irradiated p-in-n) and DUT2 (1.1×10^{13} n_{eq} cm^{-2} irradiated). In the DUT3, DUT4 and DUT5 analysis, these two track reconstruction methods, (1) and (2), were used. The median charges of various irradiated level DUTs as a function of the bias voltage are shown in Fig. 8. The bias voltage where the median charges are saturated as a function of the fluence are shown in Fig. 9. The decreases of median charges were observed after irradiation. About 4.2 fC was collected after 1.2×10^{15} n_{eq} cm^{-2} irradiation above 600 V and charge collection efficiency is about 67.7%, compared to the median charge of the unirradiated sensor which was 6.2 fC.

4.3. Plan3

Plan3 was aimed to study the length of the active region before and after irradiation. About 2M triggered events were collected for this plan. The beam tracks are reconstructed by the beam telescopes. In this analysis, the single track events, in which only one hit exists in one beam telescope plane, are used. The *X*, *Y* and *Z* shift and rotations are aligned to the position where the position resolution is minimized. The track positions are estimated to scat about 10 μm by the multiple Coulomb scattering [5] due to a low momentum beam. The hit efficiency was calculated for each 5 μm × 5 μm space point in order to study the position dependence of the hit efficiency. The collected events were categorized into single-hit and multi-hit events by cluster size. Unfortunately the tracks in the region of one side of strip edge (other side of the PTP structure) was not reconstructed at all, due to the technical problems in beam telescope during the beam test. In order to determine the precise position in *Y*, the multi-hit events are used. The hit efficiency of multi hit events is computed as the number of multi-hit events dividing by the number of all tracks. The multiple strips were overlaid on top of the one strip in order to improve the statistics. As shown in Fig. 10, the strip structure, e.g., the position of AC pads, is visible as blank area in the map, which can be used as landmarks. The double-Gaussian function, $F_{double}(x)$ shown in Eq. (4), is applied on the projection of efficiency in *Y* in order to determine the position of the pad center

$$F_{double}(x) = a_1 G(p_0 - p_1, \sigma_1) + a_2 G(p_0 + p_1, \sigma_2) + b \tag{4}$$

$$G(p,\sigma) = \frac{1}{\sqrt{2\pi\sigma^2}} \exp\left(-\frac{(x-p)^2}{\sigma^2}\right) \tag{5}$$

In these functions, p, p_0, p_1, a_1 (a_2) and b express the median, the position of the pad center, the design length between the pad center and the AC pads, the amplitude and the offset, respectively.

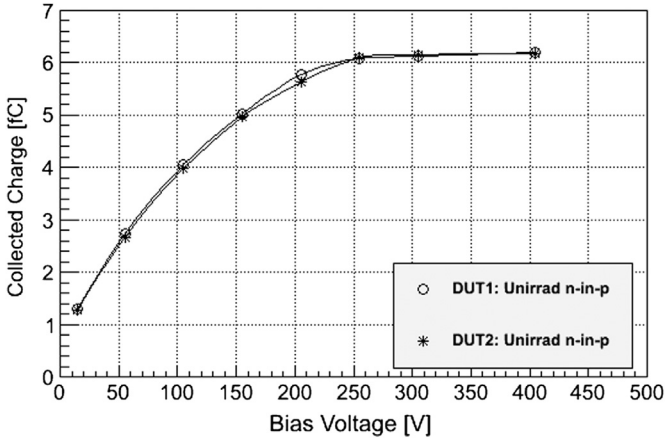

Fig. 7. The median charge vs bias voltage of un-irradiated n-in-p sensors. The behavior of DUT1 and DUT2 are almost same as expected.

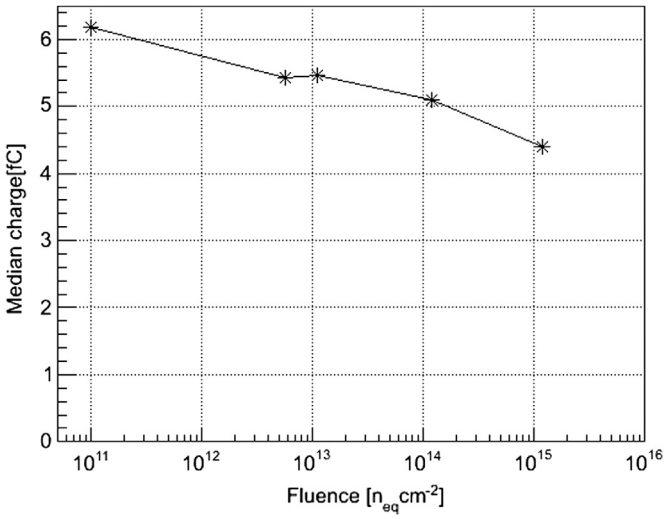

Fig. 9. The saturated median charge as a function of fluence. Median charge of un-irradiated sensor is pointed as 10^{11} n_{eq} cm^{-2}.

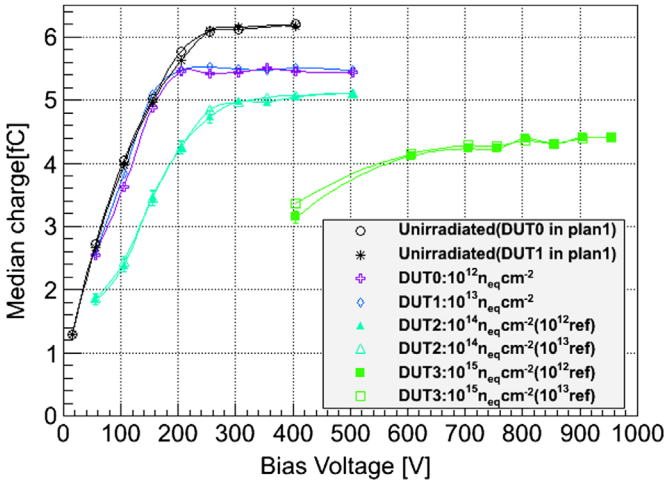

Fig. 8. The median charge as a function of sensor bias voltage. The median charges of un-irradiated sensors are about 6.2 fC while that of after 10^{15} n_{eq} cm^{-2} irradiation is about 4.2 fC.

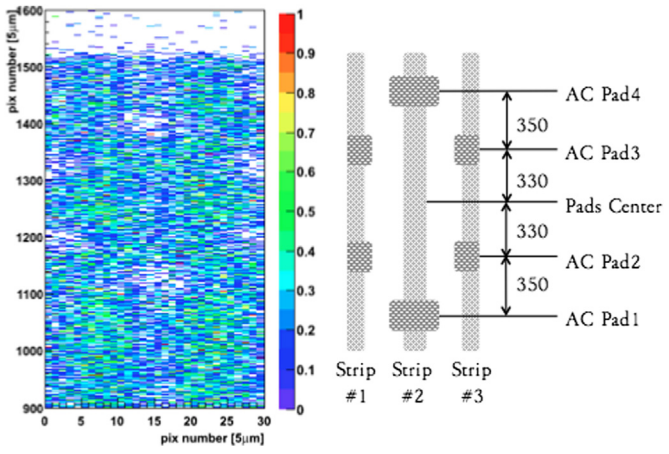

Fig. 10. Left: The hit efficiency map of multi-hit events of DUT1. Both axes are shown as the pixel number. The size of all pixel 5 μm × 5 μm. Right: The design of pad patterns of three strips. Comparing both figures, the AC pads are visible as blank area and the positions of pads are consistent with the design.

Table 3
The positions of AC pads center. Positions are calculated by applying double-Gaussian function and expressed as a pix number.

	DUT0	DUT1
# 1 & # 3 [pix number]	1292.00 ± 1.38	1264.51 ± 0.40
# 2 [pix number]	1290.10 ± 1.37	1264.88 ± 0.47
Combined	1291.05 ± 0.98	1264.70 ± 0.31
Position of active edge	1555.46 ± 0.58	1526.67 ± 0.69
Length of active region	264.98 ± 1.14	261.98 ± 0.76
Length of active region [μm]	1322.05 ± 5.68	1309.88 ± 3.78

The pad design of strips # 1 and 3 is same so that $F_{double}(x)$ applied on two patterns, # 1 & 3 and # 2. The position of the edge of the active region is calculated by fitting the projection of the hit efficiency map of all events in Y with the error function. The active length is estimated as the length from the AC pads center to the edge of the active region. The location in the design of the end of the strip and the edge of PTP gate are shown in Table 3. The design length of strip end and the edge of PTP gate is 1325 and 1316.5 μm from the pads center, respectively. A decrease in the length of the active region by 12 μm is observed. The measured active lengths are 1322.1 ± 5.7 and 1309.9 ± 3.8 μm in the un-irradiated and the irradiated samples, respectively.

5. Summary

A beam test was carried out with 394 MeV kinetic energy proton beam at RCNP in order to evaluate the n-in-p strip sensors for HL-LHC. The n-in-p miniature sensors are manufactured by HPK and sensors with various irradiation levels were tested. The new DAQ which consist of ABCN chip and SEABAS board was used in order to read-out the n-in-p sensors. The median charge of the un-irradiated n-in-p sensor saturated around 6.2 fC at 250 V, while the median charge of 1.2×10^{15} n_{eq} cm^{-2} irradiated sensor saturated around 4.2 fC at 600 V. This result shows that the charge collection efficiency of n-in-p sensors is 67.7% after 1.2×10^{15} n_{eq} cm^{-2} irradiation. The length from AC pads center to the edge of active region of un-irradiated sensor is 1322 μm, while the length of 1.2×10^{15} n_{eq} cm^{-2} irradiated sensor is 1310 μm(1309.9 μm). A decrease of the active length by 12 μm is observed. The active regions run till close to the end of the strip in the un-irradiated and to slightly before the edge of PTP gate.

Acknowledgment

The authors would like to acknowledge the staff of RCNP for the operation of the beam and the staff of KEK for technical support.

References

[1] ABC-N Asic Specification version v1.3.1, 2008.
[2] T. Uchida, Yasuo Arai, SEABAS (Soi EvAluation BoArd with Sitcp), August 2008.
[3] Y. Ikegami, et al., E383 of RCNP.
[4] The ATLAS collaboration, et al., Journal of Instrumentation 3 (2008) S08003.
[5] C. Amsler, et al., Particle Data Group, Physics Letters B 667 (1) (2008).
[6] S. Masciocchi, et al., Nuclear Instruments and Methods in Physics Research Section A 340 (1994) 572.